LATVIAN JOURNAL OF PHYSICS AND TECHNICAL SCIENCES
2015, N 3
DOI: 10.1515/LPTS-2015-0013

PHYSICS

MAGNETIC FIELD GRADIOMETER WITH SUB-MICRON SPATIAL RESOLUTION BASED ON CAESIUM VAPOUR IN AN EXTREMELY THIN CELL

M. Auzinsh[1], A. Berzins[1], R. Ferber[1], F. Gahbauer[1], U. Kalnins[1], R. Rundans[1] and D. Sarkisyan[2]

[1]Laser Centre, the University of Latvia, 19 Rainis Blvd., Riga, LV-1586, LATVIA
[2]Institute for Physical Research, NAS of Armenia, Ashtarak-0203, ARMENIA
e-mail: andris.beerzinsh@gmail.com

In this paper we present a device for measuring the magnetic field and its gradient with a spatial resolution of several hundred nanometres. This device is based on caesium metal vapour confined to an extremely thin cell (ETC). To measure magnetic signals, we use absorption and very low laser powers, which might be appealing for modern fabrication techniques. A portable, fully automated device was constructed.

Keywords: *extremely thin cell, magnetometer, measurements of magnetic field gradient, magneto-optical resonances*.

1. INTRODUCTION

Atomic vapour magnetometers have many advantages, among which are their precision and high sensitivity. Additionally, atomic magnetometers do not require cryogenic cooling, they are insensitive to spatial rotation, and they offer a significant potential for miniaturisation. Moreover, they are faster than fluxgate magnetometers. As a result, magnetometers based on gaseous species are of interest not only in physics, but also in other fields. For example, in archaeology and geophysics a set of caesium magnetometers has shown better characteristics in speed, quality, and spatial resolution than the fluxgate magnetometers [1]. In biology, caesium magnetometers have proved themselves to be as good as or even better than superconducting quantum interference devices (SQUIDs) in terms of sensitivity when measuring magnetic field changes in plants [2]. In space exploration, devices based on atomic magnetometers have great potential due to their compact size, and spin exchange relaxation-free (SERF) atomic magnetometers have already demonstrated an unsurpassed, ultra-high sensitivity of $0.54\,\mathrm{fT\,Hz^{-1/2}}$ with a measurement volume of only $0.3\,\mathrm{cm^3}$ [3]. Developments in this technology can produce sensors that can be operated on a fully optical basis [4], i.e., input and output signals in form of light using optical waveguides. In such a way, magnetic field measurements could be done in

places with strong electrical interference present. And finally, by detecting nuclear quadrupole resonance, atomic magnetometers can be used to detect dangerous or illegal substances, such as plastic explosives [5].

Nevertheless atomic magnetometers traditionally have relatively poor spatial resolution. Usually the distance between the walls of a standard spectroscopic cell is a few centimetres, or in the best case few millimetres [6], which also gives the approximate scale of achievable spatial resolution.

One way to achieve better spatial resolution is building a spectroscopy device based on an extremely thin cell (ETC). ETCs are spectroscopic cells that have two walls separated by a distance from 30nm up to several micrometres [7]. If the laser radiation propagates in the direction perpendicular to the ETC walls, most of the fluorescence will be observed from those atoms, whose velocity is small in the direction normal to the walls, since atoms flying rapidly toward an ETC wall will collide with it before being able to fluoresce. A picture of an ETC (Fig. 1) shows the interference pattern for visible light that results from the weak Fabry–Perot etalon created by the cell walls.

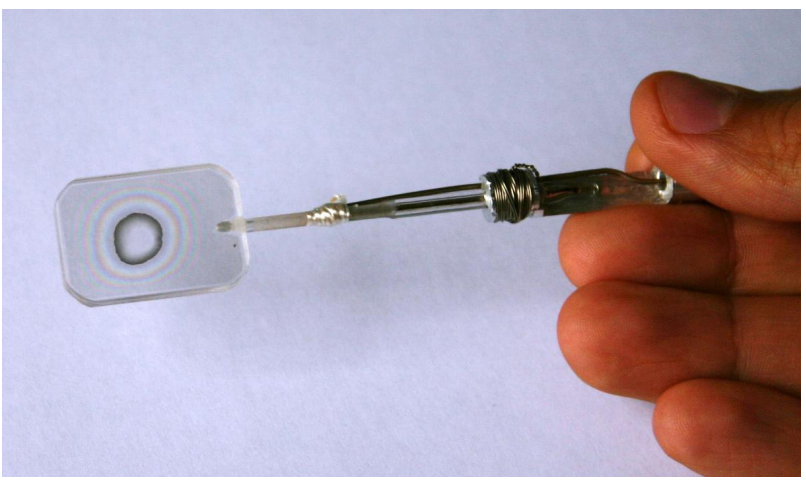

Fig. 1. A photo of ETC.

It is known that alkali metal vapours confined between walls separated by only a few hundred nanometres have the potential for applications in magnetic field measurements with elevated spatial resolution [8]. Furthermore, there is a large body of research about magneto-optical resonances (MORs) in alkali metal vapours in ordinary cells and in ETCs. For instance, nonlinear MORs have been studied experimentally and theoretically for D_1 excitation of atomic caesium, and the theoretical model [9] is successful for describing the resonances in detail [10]. Moreover, the theoretical model has proved itself by describing more complex systems with partially resolved hyperfine levels, such as the Rb D_1 and D_2 lines [11], [12], and it was in good agreement with experiments carried out in the ETC as well [13].

In this paper, we present a portable and fully automated magnetic field gradiometer with excellent characteristics in terms of spatial resolution. The device can be operated by a user without any physics training thanks to the simple-to-use software.

2 EXPERIMENTAL SETUP OF THE DEVICE

A schematic representation of the device is shown in Fig. 2. To excite the caesium atoms, we used a diode laser (Toptica DL100-DFB). A small fraction of the laser radiation was diverted from the main beam to obtain a saturation absorption (SA) spectrum in an ordinary Cs reference cell that was placed inside a three-layer mu-metal shield. The laser was stabilized to the peaks in the SA spectrum. The mu-metal shielding allowed the SA peaks to remain at fixed frequencies regardless of the magnetic field environment. Frequency stabilization was achieved by a Toptica "DigiLock 110" laser control unit, using an error signal derived from the SA spectrum. The main laser beam intensity was adjusted with a series of neutral density filters. The laser beam was focused on the extremely thin cell with a lens (f = 50 cm) and polarized with a Glan-Thompson polarizer (Thorlabs GTH10M).

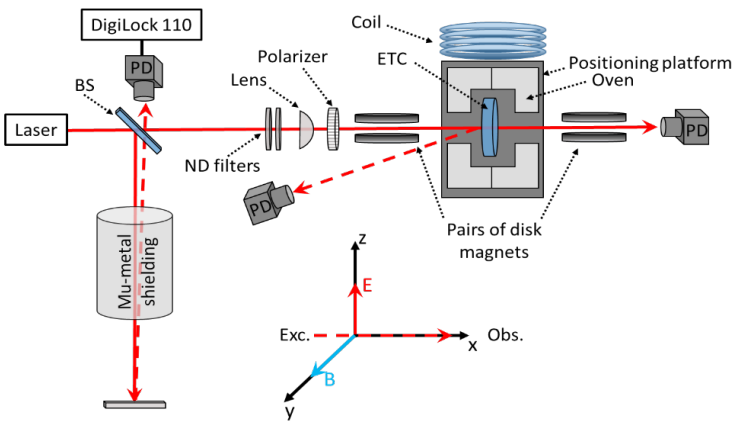

Fig. 2. Experimental setup of the device.

To achieve higher atomic density within the cell, the temperature was raised to 150°C using a small oven with bifilar heating coils to avoid generating additional fields. For the gradient measurements both the cell and the oven were mounted to a Thorlabs NanoMax positioning table, which offers a positioning resolution of 20 nm in three dimensions via voltage applied to piezo crystals. The cell position was controlled with a function generator (TTI TG5011). The absorption spectrum from the ETC was detected using a photodiode (Thorlabs PDA36-EC). The cell thickness was inferred from the interference maxima and minima in the beam reflected from the cell wall. The signals from the photodiodes were measured by a digital oscilloscope (Yokogawa DL-6154).

For the calibration of the absorption spectrum, an extra coil was added next to the oven, capable of producing a magnetic field up to 60 G. The current in the coils was produced by a bipolar power supply (Kepco BOP-50-8-M), which was controlled by another function generator (TTI TG5011). A magnetic field with a strong gradient was created around the ETC using four neodymium disk magnets.

The laser beam frequency was held constant at the *Cs* D_1 transition F_g=4 → F_e=3, where F_g stands for quantum number of full atomic angular momentum of the

ground state and F_e stands for quantum number of full atomic angular momentum of the excited state. The cell thickness was measured to be approximately 450 nm. The laser power was held at constant 5 μW with a beam diameter of 200 μm. The approximate magnetic field within the cell was from 10 G to 80 G, depending on the position. The cell was scanned over a distance of 15 μm in the direction of the laser beam with frequency of 51.4 mHz.

The dimensions of the completely assembled unit (Fig. 3) are 1.5x1x0.7 m.

Fig. 3. Completely assembled device. In the upper right part of the device one can see the optical system of the device (schematically in Fig. 2). In the left part of the device there is a PC with a monitor, keyboard, and mouse to operate the device. In the bottom right part of the device one can find power supplies, laser control units, scan generators and the positioning table control unit. All of the devices which tend to vibrate are isolated with soft plastic materials. The device is placed on a cart with wheels, which allowed it to be moved about the lab.

The measurement procedure was as follows. First, the absorption spectrum had to be calibrated. The calibration was done by scanning the magnetic field in the external coil with constant position and plotting the known magnetic field value against the absorption signal (Fig. 4). The resulting curve was fit with a fifth degree polynomial. The measurement of magnetic field gradient was done with coil turned off and the previously acquired calibration curve was then used for calculating the magnetic field values from the measured signal.

The measurement was fully computer controlled via the Virtual Instrument Software Architecture (VISA) interfaces of function generators and oscilloscope. Custom user-interface software was written for parameter input and automatisation of the calibration and measurement processes. The results of a typical measurement are shown in Fig. 5. The software allows the operator to choose the device, which will record the measurement – in our case the oscilloscope. It is possible to choose the scan generators controlling the coil and the piezo drives. There are two windows-calibration and magnetic gradient measurements. The device has default parameters

for both measurements, but they can be alternated for faster or slower measurements, different scan ranges, and level of averaging. The software allows the user to save the current measurement and load the previous ones.

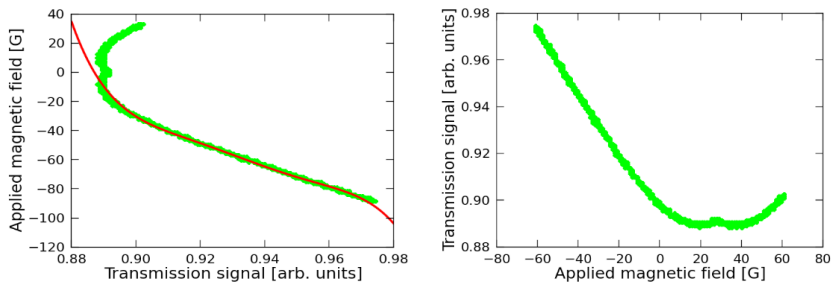

Fig. 4. Left panel – calibration signal, right panel – signal with the fitted curve, which is used to calculate magnetic field values for the gradient measurements.

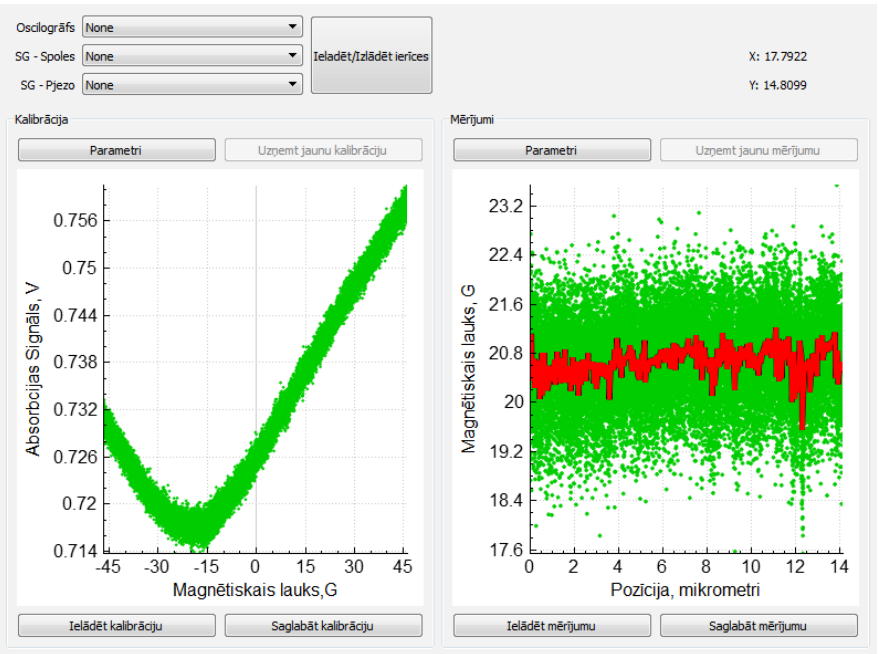

Fig. 5. Program window for measurement control. Left panel – calibration signal, right panel – magnetic field gradient measurement with one scan (blue dots), and averaged data (red line). *Note:* the red line represents the average of the measurements from one scan, not multiple scans.

3. RESULTS

By scanning the magnetic field with the coil, we get information about magnetic field values. Figure 6 shows a classical MOR with a narrow peak at zero magnetic field and rising wings at larger magnetic field values, which can be used for calibration. In Fig. 6 we can see that the zero-field resonance is reached at an applied field of approximately -30 G. From this measurement we can calibrate our gradient

measurement. In this case one must remember that even with one coil we can get a homogeneous magnetic field in the cell because the region we observe is so small that the inhomogeneity is negligible compared to measurement resolution.

In Fig. 7 a magnetic gradient measurement with averaging over multiple scans is depicted. In this graph (Fig. 7) we present a 14 μm position scan, whose absorption signal is fitted with a straight line. From this graph one can see that there is a linear magnetic field gradient over these 14 μm with the value of ~2357 G/m. The linear dependence is expected based on the fact that MORs in ETC in alkali metal vapour at elevated magnetic field values show linear dependence on magnetic field changes.

Before measuring the magnetic field, we made a simple calculation to know what magnetic field value is expected at a certain distance from the magnets. After calculating the expected magnetic field values, we made multiple scans without changes in magnetic field (i.e., ETC position) and concluded that at a magnetic field of 74 G the uncertainty in measured magnetic field values was ± 0.3 G. This gives us an error for the magnetic field measurement of 0.4%. The tested sensitivity of magnetic gradient measurement with our device was 20 mG/μm, and the accuracy with which we could detect a magnetic field gradient was about 2 mG/μm.

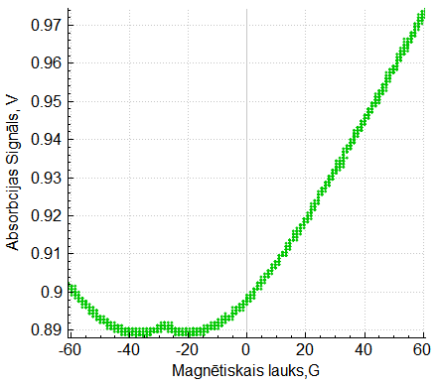

Fig. 6. Absorption signal (magneto-optical resonance) obtained for calibration.

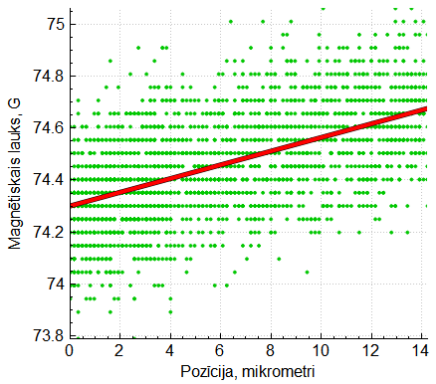

Fig. 7. Magnetic field gradient measurement (absorption signal).

4. CONCLUSIONS

Our device has proved that magnetometers on the basis of gaseous species can measure magnetic fields with outstanding spatial resolution. We have constructed a practical example for an optical magnetometer with submicron spatial resolution based on alkali metal vapours. It should be noted that the idea of using ETCs in magnetometers with outstanding spatial resolution was proposed in [7] and a laboratory device was constructed and presented in the same study. However, the device we present is portable and automated, which is the next step from a laboratory device.

With slight modifications in the system, it would be possible to measure even stronger magnetic fields. For example, a coil that can generate stronger magnetic fields could give precise calibration data for larger magnetic fields, enabling mea-

surements at magnetic field values over 100 G. Measuring near-zero magnetic fields would require additional upgrades for the software, because the linear fit for the calibration data would not be appropriate for the MOR structure at low magnetic fields. However, absorption signals in the alkali metal vapour do undergo changes near-zero magnetic field, so there are no restrictions for measuring small magnetic fields from the viewpoint of physical processes.

It should be mentioned that the system can be further improved by reducing its size – it easily could be reduced to one fourth of its starting size (many of the power supplies and control units could be replaced by smaller ones and layout of the devices could be optimized). Measurement precision could be improved by adding an additional layer of thermal isolation. Additional vibration absorbers would reduce the measurement noise. It is also possible to make measurements even at smaller distances between cell walls, but it would require longer measurement times due to the fact that layer of atoms forming the absorption signal would be even thinner.

ACKNOWLEDGEMENTS

The contribution of Artis Kruzins to the construction of the device is highly appreciated. Riga group gratefully acknowledges support from ERDF (ERAF) project no. 2010/0242/2DP/2.1.1.1.0/10/APIA/VIAA/036 "New Technology for Magnetic Field and Its Gradient Measurements Using Nanostructured Gas Environment".

REFERENCES

1. Mathé, V., Lévêque, F., and Druez, M. (2009). What interest to use caesium magnetometer instead of fluxgate gradiometer? *Mémoire du sol, espace des homes*, *33* (suppl.), 325–327.
2. Corsini, E., Acosta, V., Baddour, N., Higbie, J., Lester, B., Licht, P., Patton, B., Prouty, M., and Budker, D. (2011). Search for plant biomagnetism with a sensitive atomic magnetometer. *J. Appl. Phys. 109*, 074701, DOI:10.1063/1.3560920.
3. Kominis, I.K., Kornack, T.W., Allred J.C., and Romalis, M.V. (2003). A subfemtotesla multichannel atomic magnetometer. *Nature 422*, 596–599, DOI: 10. 1038/nature01484.
4. Patton, B., Zhivun, E., Hovde, D.C., and Budker, D. (2014). All-optical vector atomic magnetometer. *Phys. Rev. Lett. 113*, 013001, DOI:10.1103/PhysRevLett.113.013001.
5. Lee, S.-K., Sauer, K.L., Seltzer, S.J., Alem, O., and Romalis, M.V. (2006). Subfemtotesla radio-frequency atomic magnetometer for detection of nuclear quadrupole resonance. *Appl. Phys. Lett. 89*, 214106, DOI:10.1063/1.2390643.
6. Balabas, M.V., Budker, D., Kitching, J., Schwindt, P.D.D., and Stalnaker, J.E. (2006). Magnetometry with millimeter-scale anti-relaxation-coated alkali-metal vapor cells. *Journal of the Optical Society of America B. 23* (6), 1001–1006, DOI:10.1364/JOSAB.23.001001.
7. Sarkisyan, D., Bloch, D., Papoyan, A., and Ducloy, M. (2001). Sub-Doppler spectroscopy by sub-micron thin Cs vapor layer. *Opt. Commun. 200, 201,* DOI: 10.1016/S0030-4018(01)01604-2.

8. Hakhumyan, G.T. (2012). Optical magnetometer with submicron spatial resolution based on Rb vapors. *Journal of Contemporary Physics*. *47* (3), 105–112, DOI: 10.3103/S1068337212030024.
9. Blushs, K., and Auzinsh, M. (2004). Validity of rate equations for Zeeman coherences for analysis of nonlinear interaction of atoms with broadband laser radiation. *Phys. Rev. A*, *69*, 063806, DOI:10.1103/PhysRevA.69.063806.
10. Auzinsh, M., Ferber, R., Gahbauer, F., Jarmola, A., and Kalvans, L. (2008). F-resolved magneto-optical resonances in the D1 excitation of caesium: Experiment and theory. *Phys. Rev. A*, *78*, 013417, DOI: 10.1103/PhysRevA.78.013417.
11. Auzinsh, M., Ferber, R., Gahbauer, F., Jarmola, A., and Kalvans, L. (2009). Nonlinear magneto-optical resonances at D1 excitation of 85Rb and 87Rb for partially resolved hyperfine F levels. *Phys. Rev. A*, *79*, 053404, DOI: 10.1103/PhysRevA.79.053404.
12. Auzinsh, M., Berzins, A., Ferber, R., Gahbauer, F., Kalvans, L., Mozers, A., and Opalevs, D. (2012). Conversion of bright magneto-optical resonances into dark resonances at fixed laser frequency for D2 excitation of atomic rubidium. *Phys. Rev. A*, *85*, 033418, DOI:10.1103/PhysRevA.85.033418.
13. Auzinsh, M., Ferber, R., Gahbauer, F., Jarmola, A., Kalvans, L., Papoyan, A., and Sarkisyan, D. (2010). Nonlinear magneto-optical resonances at D1 excitation of 85Rb and 87Rb in an extremely thin cell. *Phys. Rev. A*, *81*, 033408, DOI:10.1103/PhysRevA.81.033408.

MAGNĒTISKĀ LAUKA GRADIOMETRS AR TELPISKO IZŠĶIRTSPĒJU ZEM MIKROMETRA, KURA DARBĪBAS PAMATĀ IR CĒZIJA TVAIKI ĻOTI PLĀNAJĀ ŠŪNĀ

M. Auziņš, A. Bērziņš, R. Ferbers, F. Gahbauers, U. Kalniņš,
R. Rundāns, D. Sarkisyan

Kopsavilkums

Šajā darbā mēs aprakstam iekārtu magnētiskā lauka un tā gradienta mērīšanai ar dažu simtu nanometru telpisko izšķirtspēju. Šīs iekārtas darbības pamatā ir cēzija metāla tvaiki, kas atrodas ļoti plānajā šūnā. Tika mērīts absorbcijas signāls, un izmantotā lāzera jauda bija ļoti zema, kas savukārt varētu būt interesanti modernām ražošanas metodēm. Pētījuma rezultātā tika izveidota portatīva un pilnīgi automatizēta iekārta.

08.04.2015.